ISSN 1068-3755, Surface Engineering and Applied Electrochemistry, 2015, Vol. 51, No. 1, pp. 76–84. © Allerton Press, Inc., 2015.

Anti-Corrosion Properties and Structural Characteristics of Fabricated Ternary Coatings[1]

O. S. I. Fayomi[a, b] and A. P. I. Popoola[a]

[a] *Department of Chemical, Metallurgical and Materials Engineering, Tshwane University of Technology, P.M.B. X680, Pretoria, South Africa*

[b] *Department of Mechanical Engineering, Covenant University, P.M.B 1034, Ota, Ogun State, Nigeria*

e-mail: ojosundayfayomi3@gmail.com, fayomio@tut.ac.za

Received October 9, 2013; in final form, November 4, 2013

Abstract—In this paper deposition of zinc (Zn)–cobalt (Co) particles and the titanium IV oxide composite (TiO_2) by electrodeposition in a single electrolyte bath was studied. Zinc coatings modified with cobalt and titanium IV oxide incorporation were produced using optimized process parameters. Morphological and microstructural properties of the fabricated coatings were characterized by an X-ray diffractometer (XRD) and a scanning electron microscope equipped with energy dispersive spectrometer (SEM/EDS). Mechanical characteristics of the coatings were evaluated by a high impact diamond-based Dura Scan micro hardness tester. The corrosion resistance properties were determined with the VA 669 PG STAT 101 using the linear potentiodynamic polarization method. As a result, it was found that the deposition of admixed Zn–Co submicron sized TiO_2 composite particles was successful. A better interfacial interaction was found to exist between the based particulate and the composite. Structural comparison of the deposited coatings with SEM, optical microscope and atomic force microscope images revealed that the homogenous grain structure was formed. Corrosion resistance increased significantly and, in addition, a better micromechanical behavior of the coatings wasattained by changing the parameters and content of Co and TiO_2 particulates.

Keywords: interface, anti-corrosion, reinforcement, structural characterization

DOI: 10.3103/S1068375515010068

INTRODUCTION

Mild steel is widely used in structural and engineering constructions due to its availability, reaso-nable cost and physical properties [1–5]. However, it has limited service performance, which is mostly caused by interactions with external media. Main environmental challenges range from chemical to mechanical interactions, depending on the service region. There are usually mechanical interactions between components in contact with each other, which tends to wear materials off. Sometimes, electrochemical responses to the environment gradually lead to lower functionality of the component because of the deterioration of its surface [5–13].

Several coating methods like vapor deposition, painting, thermal spraying, galvanizing, and systems such as zinc–iron, zinc–nickel, zinc–cobalt, chromium, aluminum have been employed over time and recently researchers have come to the verge of developing a system that can combat and strengthen the material used so that it could withstand thermal, chemical and mechanical exposure [14–18].

The discovery of nanocomposite particles for material modifications lately has become very usage for enhancement of binary formations to ternary alloys through electrodeposition. Ceramic composite based depositions are progressively used for various manufacturing applications to offer wear and hardness protection, corrosion resistance, and thermal filling [1, 19–22]. Some of these ceramics composites have a super bond matrix with ordinary functional coating particulates such as Ni–ZrO_2, Al–SiC, Ni–PZT, Ni–Al_2O_3, Cu–Al_2O_3, Zn–Al_2O_3, ZnO, TiO_2, WS_2, MoS_2, to mention but a few that have been successfully prepared and fabricated directly or indirectly through the reverse current electrodeposition [23–35].

Co and TiO_2 are in great demand for the generation of particles and composite coatings on steel and alloys with other metals [28, 33]. Zn–Co coatings are reported to have attracted greater interest due to their corrosion protection than Zn coatings; they also have characteristics similar to those of Zn–Ni. Subsequently, the potential advantage of Co addition in bath has been recognized to give resistance to abrasion and improved coating properties [28]. According to [18–20], TiO_2 composite has been effectively co-deposited with Ni, Cu, Ag and Zn. It hasnumerous

[1] The article is published in the original.

Table 1. Nominal chemical composition (wt %) of mild steel substrate

Element	C	Mn	Si	P	S	Al	Ni	Fe
Composition, %	0.15	0.45	0.18	0.01	0.031	0.005	0.008	Balance

potential engineering applications inorganic coatings, cells for photovoltaics; it contributes to catalysis, etc. Moreover, TiO_2 with a metallic coating significantly contributes to wear and corrosion resistance, better hardness [18–20, 25, 34].

With the view of the above in the present study we focus on the chemical inducement of Zn–Co–TiO_2, its microstructural, anti-corrosive and mechanical properties, when formed on mild steel substrates by electrodeposition. The produced coatings were characterized by an atomic force microscope (AFM), X-ray diffractometer (XRD) and scanning electron microscope (SEM) equipped with energy dispersive spectroscopy (EDS). Micro hardness was evaluated by the diamond-based Dura Scan micro hardness tester.

EXPERIMENTAL

Preparation of Substrates

Locally sought mild steel coupons of 40 mm × 20 mm × 1 mm were used as substrates and zinc sheets of 30 mm × 20 mm × 1 mm were used as anodes. The nominal composition (in wt %) of the mild steel plates used is given in Table 1. The cathode was of mild steel coupons and the anode was pure zinc (99.99%). The mild steel specimens were polished mechanically, degreased and immediately water washed.

Formation of Deposited Coatings

A locally prepared mild steel substrate was activated by dipping it into 10% HCl solution at room temperature for 15 seconds followed by rinsing in distilled water. Analytical grade chemicals and distilled water were used to prepare the plating solution. Prior to plating, the Co and TiO_2 particles were dispersed in the electrolyte, whose composition and parameters are presented in Table 2. The single bath formulation was then heated to about 40°C to provide a stable electrolyte and dissolve nano-particles agglomerate that might be present in the electrolytic solution as a result of a high surface capacity. The bath produced was concurrently stirred as heating lasted for hours before plating. The itinerary bath design is presented in Table 3.

Preparation of Coatings

The prepared composite admixed in a single bath after heating for 2 h and intermittent stirred to obtain clear solution first was obtained by electrolytic deposition over mild steel. Cathodes and anodes were connected to the DC power supply through a rectifier at 2 A. Electrodeposition was carried out at the applied voltage varying between 0.5–1.0 V for 15 minutes. The immersion depth was kept constant. Finally, the samples were rinsed in water to wash the salt and oxide solution off the plated samples immediately after the electroplating process.

Characterization of Coatings

The surface morphologies of the samples were investigated and the elemental analysis was performed using a TESCAN SEM–EDS and an optical microscope. The EDAX point analysis was used to trace the compositional uniformity, the phase identification of the film formed on mild steel. The topography and morphology of the samples surfaces before and after coating were studied by the AFM. The microhardness of the deposit was examined by the equal interval range indentation technique using a diamond-based Dura Scan microhardness tester. The average mean of five point's values with the 20 mm distance was recorded.

Electrochemical Characterization

The electrochemical stability behavior of the composite deposited samples was tested in 3.65 wt % NaCl solution. To study the electrochemical behavior, a conventional three-electrode cell was used, consisting of a saturated calomel electrode (SCE), graphite and

Table 2. Bath composition of ternary Zn–Co–TiO_2 alloy co-deposition

Composition	Mass concentration, g/L
ZnCl	100
KCl	50
Boric acid	10
Glycine	10
TiO_2	30
Cobalt chloride	30
Parameter	Value
pH	4.8
Voltage	0.5–1.0 V
Time	20 min
Tempt	40°C

Table 3. Itinerary bath composition of ternary Zn–Co and Zn–Co–TiO_2 alloys co-deposition

Sample number	Sample material	Time of deposition, min	Potential, V	Current, A
Blank (control)	–	–	–	–
Sample 1	Zn–TiO_2	15	1	2
Sample 2	Zn–TiO_2	15	0.5	2
Sample 3	Zn–Co–TiO_2	15	1	2
Sample 4	Zn–Co–TiO_2	15	0.5	2

coated mild steel ones used as reference, auxiliary, and working electrodes, respectively. The 1.0 cm^2 area of the working electrode was exposed to the solution and the remaining area was covered with epoxy resin, as reported in [5]. The coupons were mounted with resin and the surfaces were made to expose to the medium. The electrochemical measurement was done with an Autolab PGSTAT 101 Metrohm potentiostat/galvanostat. Other accessories were: an electrolytic cell containing 50 mL of an electrolyte, with and without a plated sample, a graphite rod which was an auxiliary electrode and a saturated calomel electrode (SCE) as a reference electrode. The potentiodynamic potential scan was fixed to run from –1.5 V to +1.5 mV, with the scan rate of 0.012 V/s. From the Tafel plots of E/I, (E_{corr}) and (j_{corr}) were evaluated.

RESULTS AND DISCUSSIONS

Morphological Studies

Figure 1a shows the surface morphology of Zn–TiO_2 co-deposits. The SEM/EDS image witnesses the dispersed harnessing of TiO_2 nanoparticles in the zinc interface. The surface structure of Zn–TiO_2 composites in the presence of glycine is also visible. The adhesion and fine grains were quite obvious, as stated in our earlier study [5]. The incorporation of TiO_2 and glycine to the electrolyte systematically influences the

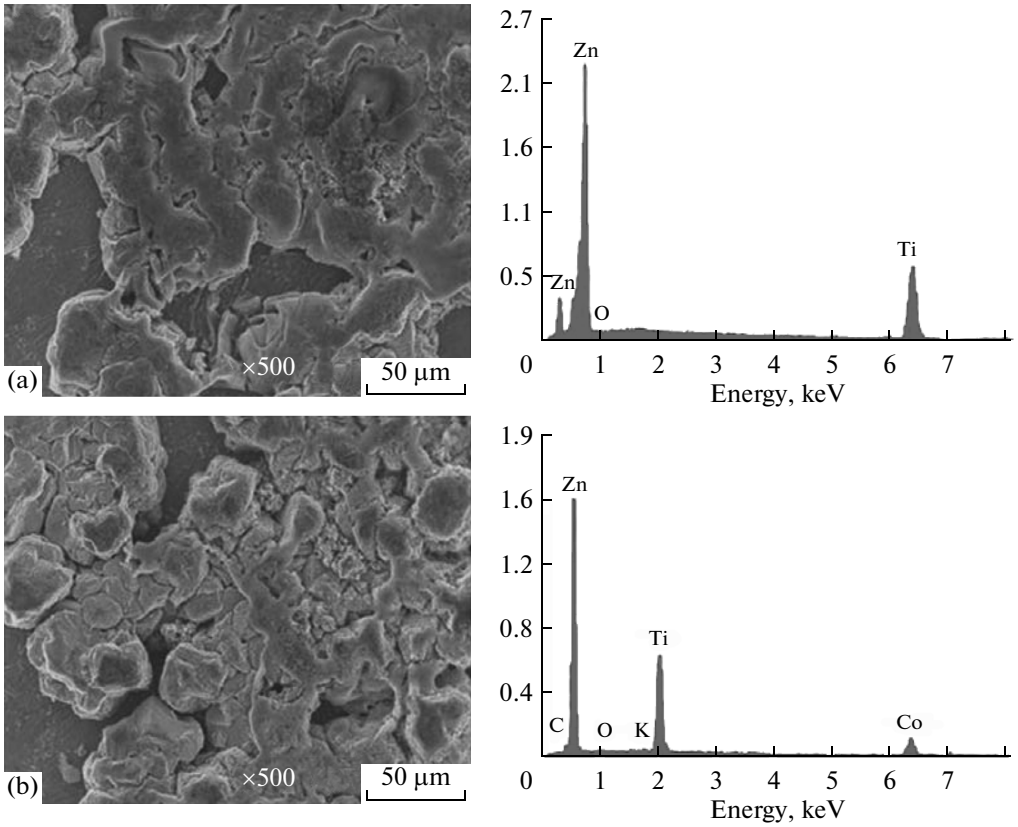

Fig. 1. SEM-EDS micrographs of: (a) Zn–TiO_2; (b) Zn–Co–TiO_2 at 1.0 V.

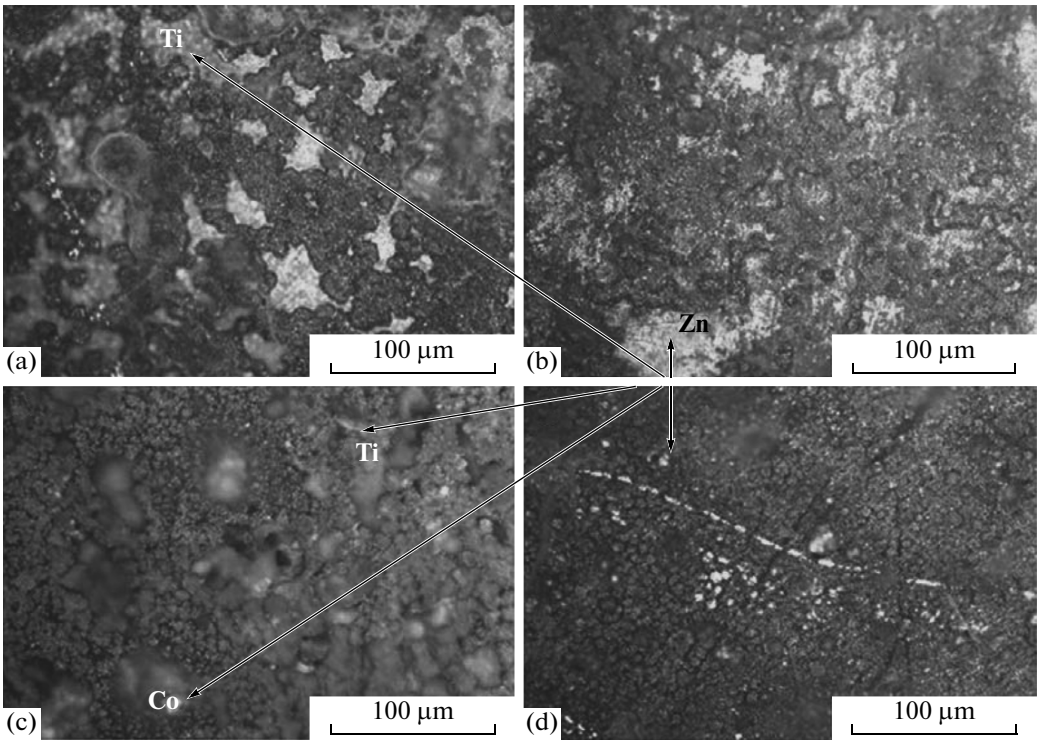

Fig. 2. Optical micrographs of: (a) Zn–TiO_2 at 0.5 V; (b) Zn–TiO_2 at 1.0 V; (c) Zn–Co–TiO_2 at 0.5 V; (d) Zn–Co–TiO_2 at 1.0 V all in 20 min.

morphological behavior giving good fine grains as a uniform blend within the matrix. The dispersion also tends to change the result of the bath to give smaller grains. A smaller grain size provides an alteration in the morphological struggle between nucleation and crystal growth [1, 2, 36].

It is reasonable to note here that the porous nature of the zinc matrix was minimized, thus providing better morphology due to the composite infiltration into the zinc bath causing adhered and uniform deposition [14, 17, 18]. In addition to this, an agglomeration within the zinc matrix might have been expected, but in this case it was different; so it is possible to assume that the factors such as a lower potential and an effect of the surfactant additive, such as glycine and the metal ion arising from adsorbing metal ion, provide strong adsorption within the particulate and the cathode [32–35].

It is worth mentioning that the fabricated Zn–TiO_2 coatings have homogenous and non-porous appearances in some areas. Hence, the crystal-shape and a smaller growth occur as an expected result and are attributed to a strong blocking effect in the zinc matrix, with EDS showing the admixed particulate being present.

Figure 1b with SEM–EDX images shows the ternary single bath Zn–Co–TiO_2 coated matrix. The grain size of the composite coated sample was smaller and more compactable when compared to that of pure Zn–TiO_2. The dramatic improvement might be due to the presence of Co incorporation into the reinforced Zn–TiO_2 composite coatings. Though the presence of TiO_2 provides more nucleation sites and decelerates the crystal growth [16–19], <1% Co has been reported in [23, 32, 33] to greatly improve the structural behavior and retard deterioration four-fold. One strange characteristic of this ternary behavior of Zn–Co–TiO_2 was a uniform and continuous thickness, without many flaws. The obvious absence of this defect and flaws along the interface is significant for the present study and is an indication of a good coating matrix and good adhesion properties. In addition to the above, the optical micrographs display the overview of some coated samples as depicted in Fig. 2.

With titanium presence in zinc rich bath a noticeable change in the surface structure in milky-white spots are observed in Fig. 2a. The crystal dispatch at the interface seems to be more visible for all depositions at 0.5 V, as seen in Figs. 2a and 2c (compare to that of a higher voltage of 1.0 V in Figs. 2b and 2d). Thus, such occurrences are expected in some cases because researchers in [2, 3] attest that lower plating potential tends to provide a better surface finish and strong adhesion.

In Figs. 2c and 2d, the grains of the deposit look smallest as affirmed in [23, 33], which is due to the suppressing action of Co in the admixed bath. At the background and interface, much more Co was found than TiO_2 particles (dark-grey spots on the optical

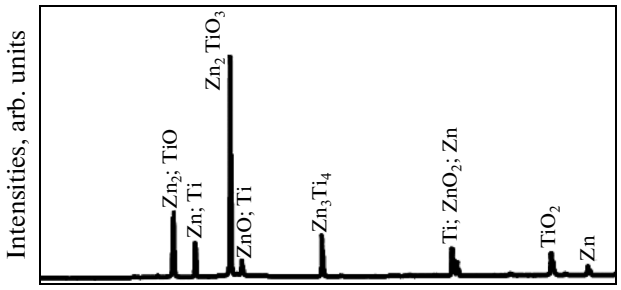

Fig. 3. XRD spectra of Zn–TiO_2 at 1.0 V.

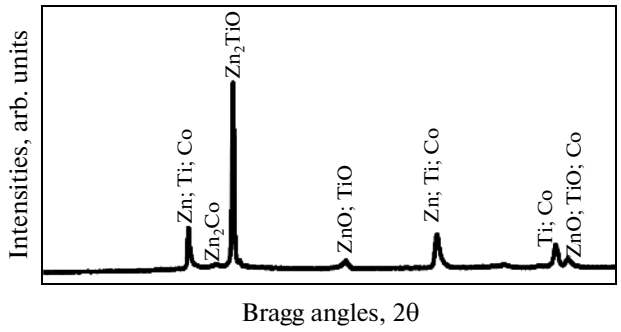

Fig. 4. XRD spectra of Zn–Co–TiO_2 at 1.0 V.

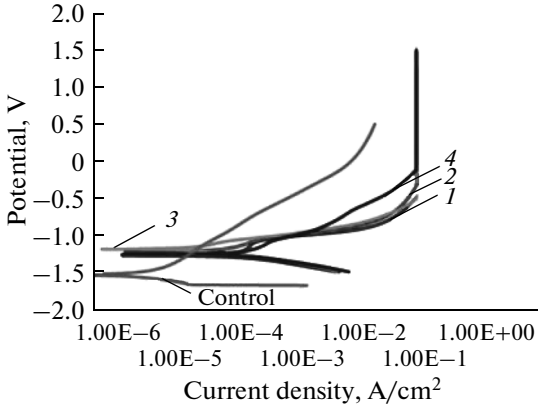

Fig. 5. Linear potentiodynamic polarization curves of coated and uncoated samples in 3.65% NaCl solution.

micrograph). Trends to the absence of porosity and good homogeneous were found with all deposits, especially with lower magnification.

XRD Phase Evaluation

Surface changes of different coated samples with Co and TiO_2 was traced for the phase analysis. Figures 3 and 4 shows the XRD spectra corresponding to the used particulate coated samples at various phases. In Fig. 3, compositions evolution of new phases, such as Zn_2Ti_2, ZnTi, Zn_3Ti_4 and Zn_2TiO, besides the original Zn-based particulate, was observed within the coated interface. Surprisingly, high strong peaks are due to the admixed particulate of Ti incorporated, resulting into co-deposition and, in turn, leading to the formation of a high-strength composite matrix.

The interaction between Zn and TiO_2 ultimately produces a crystal orientation of the grain size rather than chemical dissolution of Ti in the admixed formation. Broadening phenomenon might as well been absorbed, and, as reported in [36], to have a heavier impact in the related binary, ternary and quaternary alloys because of the presence of nano-composites.

Moreover, the influence of Co and TiO_2 resulting into the structural grain refining and modification due to the real effect and precipitation of the crystallite size by the particle addition is displayed in Fig. 4. As mentioned above, the improvement of different crystal structures can be related to the surface energy differences, which become the driving force for the relative growth of grains owing to compactness.

The presence of the intermediate dispatched composite phases observed with Zn–Co–TiO_2 series produced the highest peak with Zn_2TiO and ZnOTiOCo in its lower multiphase. However this is expected and traceable to their inter-diffusion mechanism and ion of each particulate as described by [36]. In the other hand, vivid progressions of Zn hexagonal structure from all peak diffraction line were seen, which signifies harness performance and remarkable effect of the composite induced. Since, plane intensity is due to the modification of the metal surface by the adsorption of the molecules of the composite interacting with the zinc blend of different crystal planes, which will induce different growth structure.

Hence, good blend was found to exist within the matrix intensities of the admixtures. The significant participation of Co and Ti was mostly observed at higher intensities and the morphologies of the zinc matrix improved.

Photo-Electrochemical Studies

The linear potentiodynamic polarization test was carried out in 3.65% NaCl solution. The Tafel plots acquired for the coating are shown in Fig. 5. The anodic and cathodic Tafel constants and corrosion current density values derived after extrapolation are summarized in Table 4. The positive shift of E_{corr} to −1.2256 (mV) for Zn–Co–TiO_2 at 0.5 V indicates better corrosion resistance than that of Zn–Co–TiO_2 with −1.2625 (mV) coatings at 1.0 V, as shown in Fig. 4. The same trend also holds for the binary alloy system of Zn–TiO_2 with E_{corr} of −1.2637 mV at 0.5 V, which also provides a significant improvement against plating of the fabricated alloy at 1.0 V (1.3621 mV). In all cases, the potential of the formulated and fabricated coating matrixes yielded a better improved potential

Table 4. Linear potentiodynamic polarization data of coated and uncoated samples in 3.65% NaCl solution

Sample	E_{corr}, Obs, V	j_{corr}, A/cm^2	i_{corr}, A	CR, mm/y	R_p, Ω	E, Begin, V
Sample 1	−1.2637	6.53E-05	6.53E-05	0.35239	164.76	−1.2924
Sample 2	−1.3621	2.86E-05	2.86E-05	0.75826	136.91	−1.3022
Sample 3	−1.2256	2.11E-05	2.11E-05	0.24523	413.63	−1.2509
Sample 4	−1.2625	3.03E-05	3.03E-05	0.33264	222.96	−1.2851
Control	−1.5390	7.04E-02	2.04E-03	4.10000	27.600	−1.329

than of the as-received sample at −1.3773 mV. The corrosion rate and I_{corr} subsequently followed the same trend.

From Table 4 it can be also seen that the I_{corr} value of all coated mild steel samples is by five orders of magnitude lower than of the bare mild steel. For the TiO_2 admixed coated mild steel samples at all potentials, I_{corr} are by two orders of magnitudes lower than of the as-received sample. The beneficial effect of Co and TiO_2 in the improvement of the corrosion resistance of this Zn-based coating may be due to a strong activity and affinity between Co, TiO_2 and Zn, which is responsible for the development of a synergistic effect, while improving the corrosion resistance of the ternary coated mild steel.

So, the coatings improved the corrosion resistance of the mild steel substrate, adding to it a significant polarization resistance. This indicates that the admixed coating matrixes are promising as the substrate material but must be restrained to a certain potential of a coating to enforce compactness and cohesion.

Although the resistance behavior of materials certainly influences the corrosion rate [31–33], the polarization resistance of all of the coated samples was greatly improved in the following order: 3 > 4 > 1 > 2 > Blank (control), with the R_p values of 413.63 Ω, 222.96 Ω, 164.76 Ω, 136.91 Ω, and 27.600 Ω, respectively. This tendency is attributed to the oxidation noticed on the surface of the modified coating. A more positive shift in the corrosion potential was found with Zn–Co–TiO_2, having R_p of 413.63 Ω.

Figures 6a–6d show the optical images of Zn–TiO_2 at 0.5 V, Zn–TiO_2 at 1.0 V, Zn–Co–TiO_2 at 0.5 V, and

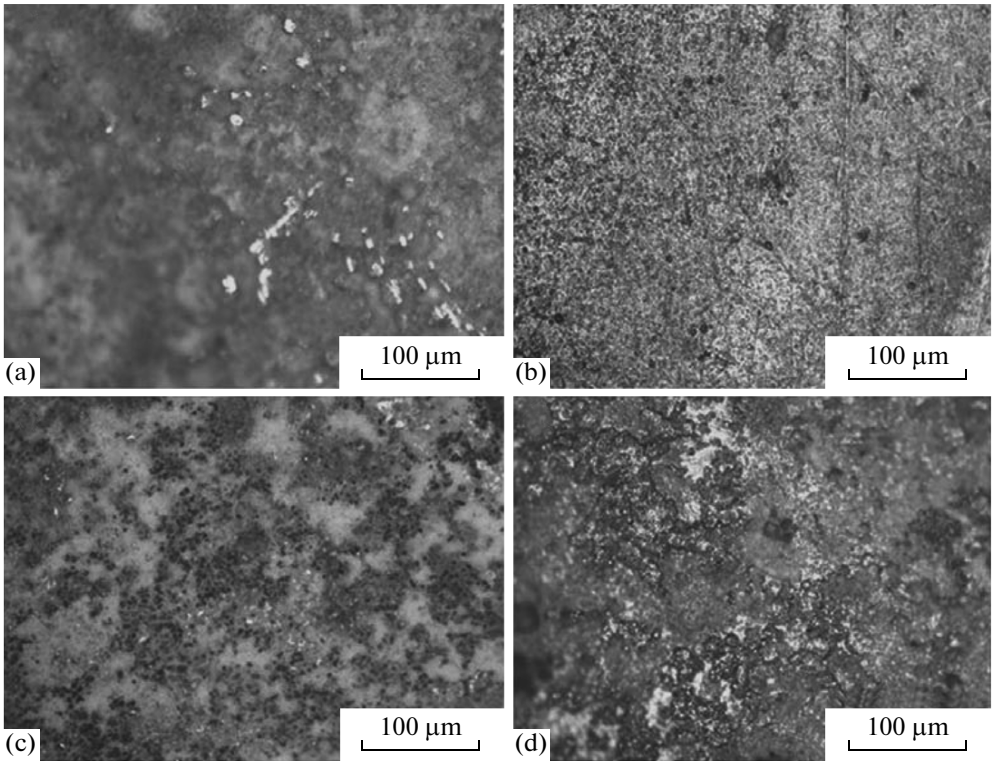

Fig. 6. OPM analysis of: (a) Zn–TiO_2 at 0.5 V; (b) Zn–TiO_2 at 1.0 V; (c) Zn–Co–TiO_2 at 0.5 V and (d) Zn–Co–TiO_2 at 1.0 V after corrosion.

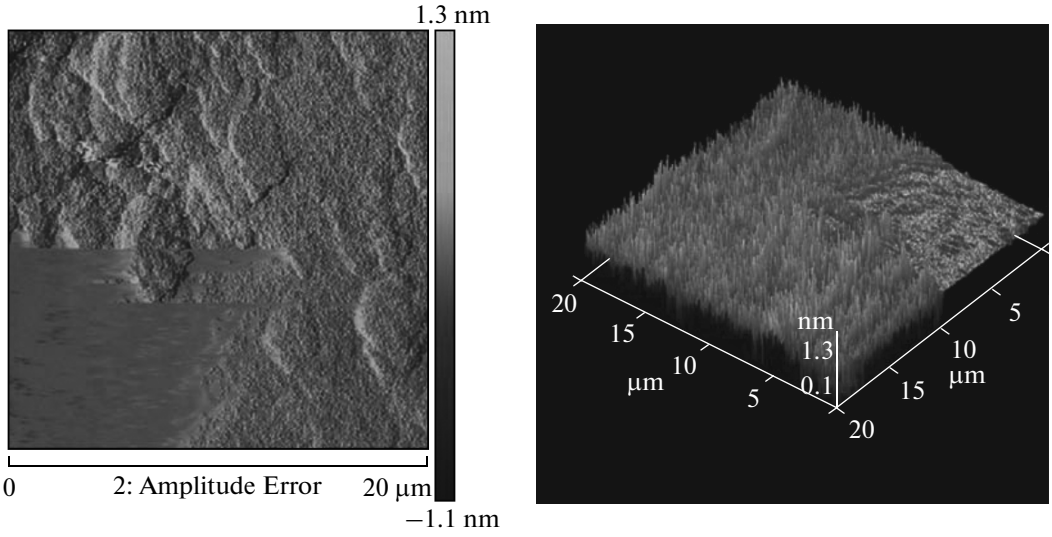

Fig. 7. AFM micrographs of: Zn–TiO_2 at 0.5 V.

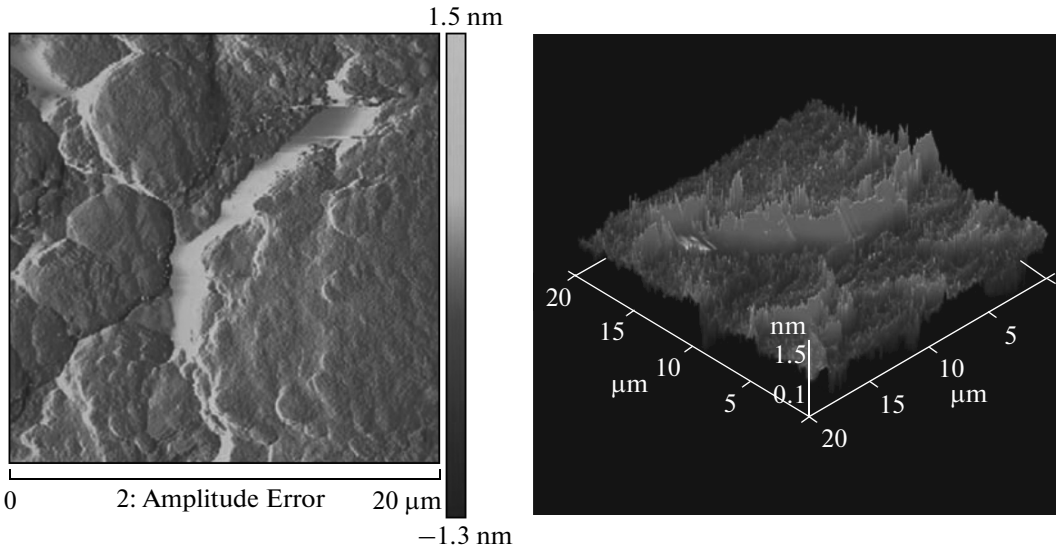

Fig. 8. AFM micrographs of Zn–Co–TiO_2 at 0.5 V.

Zn–Co–TiO_2 at 1.0 V, after corrosion in the 3.65% NaCl solution. In general, all coated surfaces still look satisfactory even after corrosion examination. Those appreciable corrosion products were observed as white and darker spots. In the case of a composite coated samples, with Co admixed, the size of these products was minimal, with the homogenous corrosion occurrence. Generally, the TiO_2 inclusion in the zinc deposit brings down the corrosion rate, thus reducing the metal loss.

The overall optical micrograph studies establish that the zinc-titanium coated surfaces have less corrosion products at the interface. The degree of the corrosion-caused deterioration was not visible at all for Zn–Co–TiO_2. This indicates the effect of the Zn–Co–TiO_2 adhesion coated samples that have higher resistance to corrosion; those data were systematically compared to the results obtained by SEM studies.

AFM Analysis

The AFM was used to make an analysis of Zn–TiO_2 and Zn–Co–TiO_2, both obtained at 0.5 V, as shown in Figs. 7 and 8. In both alloys deposited, a uniform crystallites coalesced with small grains were found affirming the morphological result obtained by SEM. The topography of Zn–Co–TiO_2 shows some undulation which expectedly might arise as a results of Co incorporation into the Zn–TiO_2 matrix. The undulation progression within the interface by the additive might

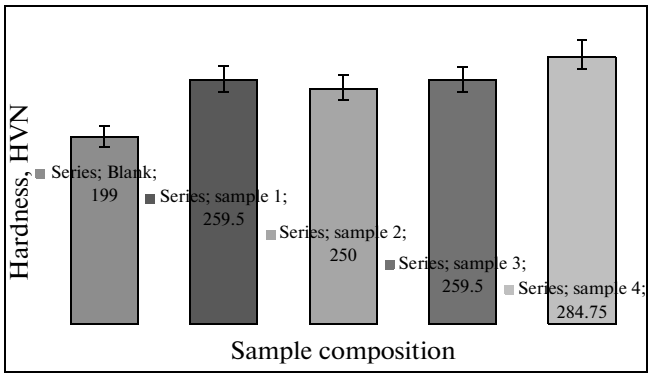

Fig. 9. Variations of micro-hardness of: sample 1—Zn–TiO_2 at 0.5 V; sample 2—Zn–TiO_2 at 1.0 V; sample 3—Zn–Co–TiO_2 at 0.5 V, and sample 4—Zn–Co–TiO_2 at 1.0 V, all in 20 min.

also necessitate the adhesion behavior of the coated alloys.

Microhardness Studies

Figure 9 visualizes the effects of TiO_2 and Co on the Zn interface at the applied voltage of 0.5 and 1.0 V. From all indicators, the microhardness rises with an additive dispersed into the bath. A pronounced microhardness change was noticed for samples 3 and 4 that contain the Zn–Co–TiO_2 matrix at their applied potential, suggesting the Co strengthening effect. Reports in [4, 5] tell us that ceramics composite particles can lead to refinement in the grain structure and improve the microhardness of the composite coatings. Thus the TiO_2 composite changes cause smaller grains and provide structural modifications, which could enhance the hardness of the composite coatings [19, 27, 30]. Moreover, Co was attested to have compatibility properties in bath and its presence in the composite coatings improved their mechanical properties [23, 33].

In line with the results, both Co and TiO_2 particulate contribute immensely to the hardness behavior of the Zn–TiO_2 and Zn–Co–TiO_2 coatings; hence the absence of cracks and flaws, as earlier stated, is a prerequisite for the fabrication of a well adhered coating with good hardness properties. The coating alloys have a homogeneous composition, which shows there is no deleterious effect of the cracked morphology on the hardness properties. A significant difference could be seen from 199 Hv, in as-received samples, to 284 Hv, in as-observed ones, for sample 4 (Zn–Co–TiO_2) matrixes.

CONCLUSIONS

• In this work, mixed Co–TiO_2 films have been successfully deposited on mild steel substrates by electrolytic co-deposition. The alloy of Zn–Co–TiO_2 has been introduced to replace the Zn–TiO_2 and Zn–Co alloys in coatings.

• XRD results of the deposits have shown that the Zn–Co–TiO_2 alloy coatings consisted of Zn_2Co, Zn_2Ti, ZnTiCo and ZnCo 13 phases.

• The Zn–Co–TiO_2 coatings showed better adhesion strength compared to that of Zn–TiO_2 alloy coatings.

• In general, from the morphological, mechanical and electrochemical studies, Zn–Co–TiO_2 alloy coatings have shown better performance than Zn–TiO_2, in terms of displaying a trend for homogeneous diffusion and good interfacial properties. With the presence of Co, a wide application can be the base for commercialization.

ACKNOWLEDGMENTS

This work was financially supported by the National Research Foundation of South Africa. The laboratory imputes of Surface Engineering Research Centre (SERC) is appreciated.

REFERENCES

1. Tiwari, S.K., Sahu, R.K., Pramanick, A.K., and Singh, R., Development of conversion coating on mild steel prior to sol gel nanostructured Al_2O_3 coating for enhancement of corrosion resistance, *J. Surf. Coat. Technol.*, 2011, vol. 205, pp. 4960–4967.
2. Popoola, A.P.I., Fayomi, O.S.I., and Popoola, O.M., Electrochemical and mechanical properties of mild steel electroplated with Zn–Al, *Inter. J. Electrochem. Sci.*, 2012, vol. 7, pp. 4898–4917.
3. Popoola, A.P.I., Fayomi, O.S.I., and Popoola, O.M., Comparative studies of microstructural, tribological and corrosion properties of plated Zn and Zn-alloy coatings, *Inter. J. Electrochem. Sci.*, 2012, vol. 7, pp. 4860–4870.
4. Fayomi, O.S.I. and Popoola, A.P.I., An investigation of corrosion and mechanical behavior of Zn coated mild steel in 3.65% NaCl, *Inter. J. Electrochem. Sci.,* 2012, vol. 7, pp. 6555–6570.
5. Lekka, M., Kouloumbi, N., Gajo, M., and Bonora, P.L., Corrosion and wear resistant electrodeposited composite coatings, *Electrochem. Acta*, 2005, vol. 50, pp. 4551–4556.
6. Ciubotariu, A., Benea, L., Varsanyi, M., and Dragan, V., Electrochemical impedance spectroscopy and corrosion behavior of Al_2O_3–Ni nano-composite coatings, *Electrochem. Acta*, 2008, vol. 53, pp. 4557–4563.
7. Hammami, O., Dhouibi, L., and Triki, E., Influence of Zn–Ni alloy electro-deposition techniques on the coating corrosion behavior in chloride solution, *Surf. Coat. Technol.*, 2009, vol. 203, pp. 2863–2870.
8. Panagopoulos, C.N., Georgiou, E.P., Tsoutsouva, M.G., and Krompa, M., Composite multilayered coatings on mild steel, *J. Coat. Technol. Res.*, 2011, vol. 8, pp. 125–133.

9. Fayomi, O.S.I. and Popoola, A.P.I., Chemical interaction, interfacial effect and the microstructural characterization of the induced zinc–aluminum–solanum tuberosum in chloride solution on mild steel, *Research on Chemical Intermediates*, 2013, vol. 39, no. 6, DOI 10.1007/s11164-013-1354-2.
10. Changa, L.M., Chena, D., Liub, J.H., and Zhang, R.J., Effects of different plating modes on microstructure and corrosion resistance of Zn–Ni alloy coatings, *J. Alloy Comp.*, 2009, vol. 479, pp. 489–93.
11. Cotell, C.M., Sprague, J.A. and Smidt, F.A., *ASM Metals Handbook. Surf. Eng.*, 1999, vol. 5, p. 804.
12. Ger, M.G. and Grebe, R., Electrochemical deposition of Nickel/SiC composites in the presence of surfactants, *Mater. Chem. Physic.*, 2004, vol. 87, no. 1, pp. 67–74.
13. Gay, P.A., Bercot, P., and Pagetti, J., Electro-deposition and characterization of Ag–ZrO_2 electroplated coatings, *Surf. Coat. Technol.*, 2001, vol. 140, no. 2, pp. 147–154.
14. Sancakoglu, O., Culha, O., Toparli, M., Agaday, B., and Celik, E., Co-deposited Zn-submicron sized Al_2O_3 composite coatings: Production, characterization and micromechanical properties, *Mater. Design*, 2011, vol. 32, pp. 4054–4061.
15. Yao, Y., Yao, S., Zhang, L., and Wang, H., Electro-deposition and mechanical and corrosion resistance properties of Ni–W/SiC nano-composite coatings, *Mater. Letter*, 2007, vol. 61, no. 1, pp. 67–70.
16. Chen, X.H., Chen, C.S., Xiao, H.N., Cheng, F.Q., Zhang, G., and Yi, G.J., Corrosion behavior of carbon nanotubes–Ni composite coating, *Surf. Coat. Technol.*, 2005, vol. 191, nos. 2–3, pp. 351–356.
17. Praveen, B.M., Venkatesha, T.V., Arthoba Naik, Y., and Prashantha, K., Corrosion studies of carbon nanotubes–Zn composite coating, *Surf. Coat. Technol.*, 2007, vol. 201, no. 12, pp. 5836–5842.
18. Praveen, B.M., Venkatesha, T.V., Naik, Y.A., and Prashantha, K., Corrosion behavior of Zn–TiO_2 composite coating, *Syn. React. Inorg. Met.*, 2007, vol. 37, no. 6, pp. 461–465.
19. Gomes, A., Almeida, I., Frade, T., and Tavares, A.C., Zn–TiO_2 and ZnNi-TiO_2 Nano-composite coatings: Corrosion behavior, *Mater. Sci. Forum*, 2010, vols. 636–637, pp. 1079–1083.
20. Prashantha, K. and Park, G.S., Nano-sized TiO_2-filled sulfonated polyethersulfone proton conducting membranes for direct methanol fuel cells, *J. Appl. Polym. Sci.*, 2005, vol. 98, no. 5, pp. 1875–1878.
21. Sachin, H.P., Achary, G., Arthoba Naik, Y., and Venkatesha, T.V., Polynitroaniline as brightener for zinc-nickel alloy plating from non-cyanide sulphate bath, *Bull. Mater. Sci.*, 2007, vol. 30, no. 1, pp. 57–63.
22. Shibli, S.M.A., Dilimon, V.S., Antony, S.P., and Manu, R., Incorporation of TiO_2 in hot dip zinc coating for efficient resistance to bio-growth, *Surf. Coat. Technol.*, 2006, vol. 200, nos. 16–17, pp. 4791–4796.
23. Mahieu, J., De Wit, K., De Boeck, A., and De Cooman, B.C., The properties of electrodeposited Zn–Co coatings, *J. Mater. Eng. Perform.*, 1999, vol. 8, pp. 561–570.
24. Fayomi, O.S.I., Tau, V.R., Popoola, A.P.I., Durodola, B.M., Ajayi, O.O., Loto, C.A., and Inegbenebor, O.A., Influence of plating parameter and surface morphology on mild steel, *J. Mater. Environ. Sci.*, 2011, vol. 3, pp. 271–280.
25. Fustes, J., Gomes, D.A., and Pereira, M.I.S., Electrodeposition of Zn–TiO_2 nano-composite films-effect of bath composition, *J. Solid State Electrochem.*, 2008, vol. 121, no. 11, pp. 1435–1443.
26. Mohankumar, C., Praveen, K., Venkatesha, V., Vathsala, K., and Nayana, O., Electro-deposition and corrosion behavior of Zn–Ni and Zn–Ni–Fe_2O_3 coatings, *J. Coat. Technol. Res.*, 2012, vol. 9, no. 1, pp. 71–77.
27. Praveen, B.M. and Venkatesha, T.V., Electro-deposition and corrosion resistance properties of Zn–Ni/TiO_2 nano-composite coating, *Inter. J. Electrochem.*, 2011, vol. 261, pp. 407–410.
28. Dikici, T., Culha, O., and Toparli, M., Study of the mechanical and structural properties of Zn–Ni-Co ternary alloy electroplating, *J. Coat. Technol. Res.*, 2010, vol. 7, no. 6, pp. 787–792.
29. Byk, T.V., Gaevsaya, T.V., and Tsybulskaya, O., Effect of electro-deposition conditions on the composition, microstructure, and corrosion resistance of Zn–Ni alloy coatings, *Surf. Coat. Technol.*, 2008, vol. 202, no. 24, pp. 5817–5823.
30. Praveen, B.M. and Venkatesha, T.V., Electro-deposition and properties of Zn-nano-sized TiO_2 composite coatings, *Appl. Surf. Sci.,* 2008, vol. 254, no. 8, pp. 2418–2424.
31. Fayomi, O.S.I., Abdulwahab, M., and Popoola, A.P.I., Properties evaluation of ternary surfactant-induced Zn–Ni-Al_2O_3 films on mild steel by electrolytic chemical deposition, *J. of Ovonic Research*, 2013, vol. 9, no. 5, pp. 123–132.
32. Popoola, A.P.I. and Fayomi, O.S., Effect of some process variable on zinc coated low carbon steel substrates, *Sci. Res. Essay.*, 2011, vol. 6, pp. 4264–4272.
33. Basavanna, S. and Arthoba Naik, Y., Electrochemical and reflectance studies of bright Zn–Co alloy coating, *J. Appl. Electrochem.*, 2012, vol. 517, no. 11, pp. 3287–3291.
34. Vasilyeva, M.S., Rudnev, V.S., Korotenko, I.A., and Nedozorov, P.M., Production and studying oxide coatings containing manganese and nickel compounds on titanium from electrolyte suspensions, *Protection of Metals and Physical Chemistry of Surfaces*, 2012, vol. 48, no. 1, p. 106.
35. Zhou, Q., Shao, Z., He, C., Shao, Z., Cai, Q., and Gao, W., Impact of surfactants on electro less deposition Ni–P-nano-Al_2O_3 composite coating, *J. of the Chinese Society of Corrosion and Protection*, 2007, vol. 27, no. 1, pp. 27–30.
36. Ranganatha, S., Venkatesha, T.V., Vathsala, K., and Punith Kumar, M.K., Electrochemical studies on Zn/nano-CeO_2 electrodeposited composite coatings, *Surf. Coat. Technol.*, 2012, vol. 208, pp. 64–72.